Temperature Evolution, Microstructure and Mechanical Properties of Heat-Treatable Aluminum Alloy Welded by Friction Stir Welding: Comparison with Tungsten Inert Gas

Saliha Gachi, Mouloud Aissani, Fouad Boubenider

Abstract—Friction Stir Welding (FSW) is a solid-state welding technique that can join material without melting the plates to be welded. In this work, we are interested to demonstrate the potentiality of FSW for joining the heat-treatable aluminum alloy 2024-T3 which is reputed as difficult to be welded by fusion techniques. Thereafter, the FSW joint is compared with another one obtained from a conventional fusion process Tungsten Inert Gas (TIG). FSW welds are made up using an FSW tool mounted on a milling machine. Single pass welding was applied to fabricated TIG joint. The comparison between the two processes has been made on the temperature evolution, mechanical and microstructure behavior. The microstructural examination revealed that FSW weld is composed of four zones: Base metal (BM), Heat affected zone (HAZ), Thermo-mechanical affected zone (THAZ) and the nugget zone (NZ). The NZ exhibits a recrystallized equiaxed refined grains that induce better mechanical properties and good ductility compared to TIG joint where the grains have a larger size in the welded region compared with the BM due to the elevated heat input. The microhardness results show that, in FSW weld, the THAZ contains the lowest microhardness values and increase in the NZ; however, in TIG process, the lowest values are localized on the NZ.

Keywords—Friction stir welding, tungsten inert gaz, aluminum, microstructure.

I. INTRODUCTION

FSW is a solid state joining method applied to join aluminium alloys, which are difficultly weldable by fusion process. The maximum temperature reached in this process is around 80% of the melting temperature as reported by Tang et al. [1] and Colegrove et al. [2], so that welding defects and large distortion usually related to the fusion process are minimized or avoided. The main advantages of this solid phase process consist of: joining aluminium sheets/plates without filler wire or shielding gas, avoiding severe distortions, reducing the generated residual stresses [3], [4]. Moreover, this process needs less energy for joining and the maximum peak temperature is lower compared to conventional arc weldments with a better preservation of original mechanical properties, for these reasons, this technique is attracting an increasing amount of research interests.

The FSW process uses a specially designed cylindrical rotating, non-consumable tool with in particular two essential conventional parts, "shoulder and pin". The design of shoulder and pin is very important for the weld quality. The rotating tool causes local changes in the welded material because of mechanical deformations and heat transfer. It is plunged into the abutting edges of plates to be welded to achieve its two principal functions: (a) heating of workpieces and (b) stirring of material to produce the joint [5], [6]. The shoulder applies a pressure under rotation on the material to constrain the plasticized material around the pin.

The tool geometry, such as the height, the pin shape and the shoulder surface have a great influence on both the metal flow and the heat generation due to friction forces. Also, the forging force applied on the FSW tool during the process has to be properly chosen, since the pressure generated on the tool shoulder surface and under the pin end determines the heat generated during the process [7], [8].

Another important factor that has an impact on both the weld microstructure, residual stresses evolution and consequently the mechanical properties of the weld is the peaks temperature. Insufficient weld temperatures prevent the weld material to well accommodate the extensive plastic flow during welding and require more force action of the tool. So, tunnel defects can occur along the weld subsurface. Low temperatures may also limit the tool penetration and so reduce the continuity of the attachment between the materials from each side of the weld. The light contact between the materials has known as kissing bond defect [9], [10].

In order to promote and confirm the performance and the potentialities of the FSW technique to join light and high strength material used heavily in aerospace industry, such as 2024-T3 Aluminium alloy, a comparison has been made between this solid state process and a fusion state one; it is the conventional TIG. In TIG welding, an electric arc is formed between non-consumable tungsten electrode and the workpiece. This arc provides the thermal energy to melt the workpieces as well as the filler metal if necessary; the weld region is protected by the argon shielding gas against the air oxidation. The comparison between the two processes has

Saliha Gachi is with the Laboratory of physics and materials, University of Science and Technology Houari Boumediene (USTHB), BP32 El Alia Bab Ezzouar, Algiers, Algeria (e-mail: s_gachi@yahoo.fr).

Fouad Boubenider is with the Laboratory of physics and materials, University of Science and Technology Houari Boumediene (USTHB), BP32 El Alia Bab Ezzouar, Algiers, Algeria.

Mouloud Aissani is with the Research Center in Industrial Technologies CRTI, BP 64, Cheraga 16014 Algiers, Algeria.

been made in terms of temperature evolution, mechanical, SEM and microstructure characterizations.

II. EXPERIMENTAL LAYOUT

In this study, 2024-T3 aluminium alloy sheets were friction stir welded in the butt joint configuration. The concentration of the basic elements is given in Table I.

TABLE I
CONCENTRATIONS OF CUPPER AND MAGNESIUM PRESENT IN 2024-T3 ALUMINIUM ALLOY

Element	O	Cu	Mg	Al
% on weight	02.75	04.60	00.93	91.73
% on atomic	04.66	01.97	01.04	92.33
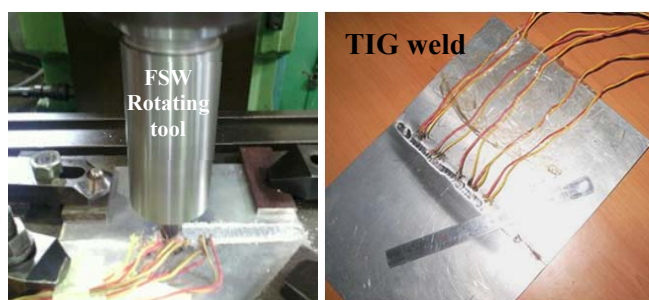
Fig. 1 Experimental set up for thermal characterization in FSW and TIG welds

TABLE II
THERMOCOUPLES' IMPLANTATION COORDINATES

	Thermocouples #	Tc_1	Tc_2	Tc_3	Tc_4	Tc_5	Tc_6
FSW	X Position (mm)	13	16	13	18	13	20.5
	Y Position (mm)	76	72	98	94.5	115	115
TIG	X Position (mm)	3	4.5	5	5.5	8	12
	Y Position (mm)	40	55	75	90	100	120

The shoulder and pin diameters are fixed and equal to 20 and 6 mm, respectively. The pin length is approximately 0.3 mm which is less than the sheets thickness to avoid any contacting with the anvil. The tool is mounted in a conventional vertical milling machine.

A comparison has been made between this innovative solid-state welding process (FSW) and the traditional TIG process. The TIG welding for the same alloy has been joined without filler metal. Detailed welding parameters are: voltage of 15V, current of 59A, argon as shield gas (flow rate 7 l/min), electrode diameter of 1.20 mm and welding speed of 1.6 mm s^{-1}.

It is important to obtain information about temperature evolution during the welding. For this, a specific assembly is carried out, using a thermal recorder of high frequency registration (FLUKE 26381 Hydra Data Logger) and thermocouples of "K" kind. These thermocouples can support temperatures from -40 to 1200 °C and are connected to the thermal recorder. Temperatures were logged by thermocouples located on the regions adjacent to the rotating tool path at various distances from the weld centerline. For TIG weld, the thermocouples were placed on region adjacent to the weld line

(Fig. 1). The thermocouples' implantation coordinates for FSW and TIG processes are given in Table II. The longitudinal direction Y is parallel to the welding direction, so the transverse direction X is perpendicular to Y.

For the microstructural examination, the welded sheets are cut up perpendicular to the welding direction, polished, and etched with chemical product type 'Keller's reactive in ambient temperature. The micrographics results are obtained using an optical microscope "AXIOPLAN (ZEISS)" equipped with a numerical camera and image analyzing software MR GRAB. The Vicker's microhardness data are obtained across the weld for the different zones, using a microhardness tester with a test load of 300 g and step of 0.5 mm, on polished weld surface. The fractured surfaces were analyzed using scanning electron microscope (SEM) in order to highlight the rupture mode.

III. RESULTS AND DISCUSSIONS

The experimental thermal cycles obtained during FSW welding are given in Fig. 2. It is observed that the overall appearance of the curves (cycles) is the same for the six thermocouples; such as the temperature increases rapidly by passing through a maximum, then decreases in cooling phase over time in different speeds to reach the ambient temperature. The maximum temperatures were recorded at distances close to the stirred zone (Tc_1, Tc_3 and Tc_5) and are about 301±3 °C. They decreased with increasing distance from the weld center line (Tc_2, Tc_4 and Tc_6). The minimum peak reached is about 239 °C on Tc_6 position that corresponds to the HAZ region. Furthermore, the thermal cycle shows faster cooling after welding, this is explained by the heat transfer effect between the welded sheets and the anvil. Similar remarks were observed by Hugh et al. [11] in their experiment on AA2024-T3 alloy using a range of experimental and numerical (finite element) thermal model. Moreover, the maximum temperature within the stirred zone is higher than that measured in the regions close to the stirred one and lower than the melting point of 2024-T3 because no material melting was observed in the FSW weld.
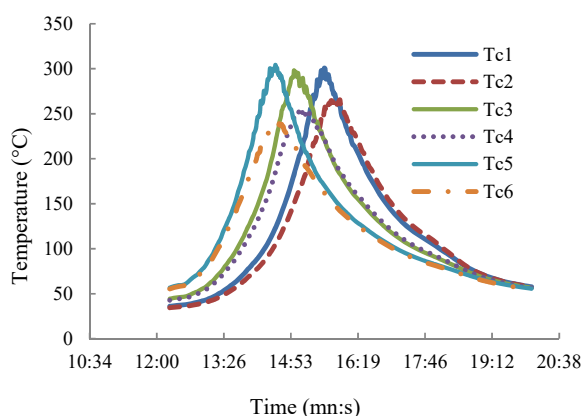

Fig. 2 Experimental thermal cycles of 2024-T3 welded by FSW

Fig. 3 that shows the experimental thermal cycles for TIG process illustrate that experimental thermal cycles profile is the same as found previously for FSW weld but the heating and cooling rate are higher in TIG process than in FSW. Note that the maximum temperature value recorded in the closest distance to the weld zone (Tc_1) is around of 518 °C. For the same thermocouple position, the temperature peak recorded in TIG process (Tc_5) is equal to 403 °C and in FSW process (Tc_1) is around 301 °C. The temperature difference of 102 °C is noted between the two cycles. Therefore, FSW allows a reduction of about 25% in temperature level compared to TIG welding. The experimental thermal cycles obtained confirm the literature notification [12]; the temperatures reached in TIG welding are very higher compared to FSW.
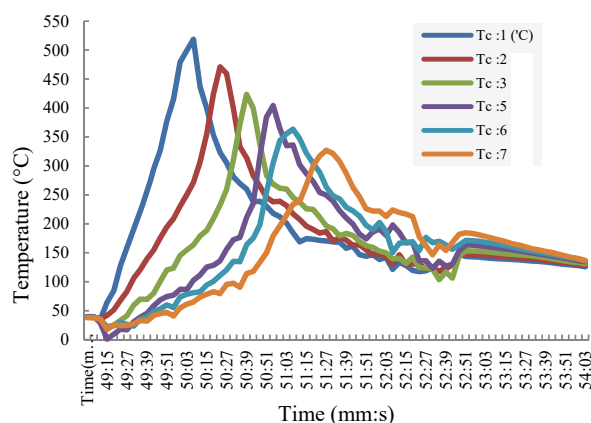
Fig. 3 Experimental thermal cycles of 2024-T3 welded by TIG process

Fig. 4 shows the microhardness distribution over the FSW weld cross section. The average microhardness of BM is 132 HV. In the welded joint, the microhardness varies greatly over the weld forming the "W" profile. This variation is most important especially in the HAZ where the minimal value reached is 80 HV. This value remains weak in the TMAZ with some fluctuations. These lowest values are due the growth and coalescence of precipitates that lose their coherence within the matrix because of the high temperatures and mixing effects. In the NZ, the microhardness increase is approximately equal to 110 HV. This is mainly due to the formation of very fine grains in this zone caused by severe plastic deformation and very high temperature during friction stirring. This phenomenon is known as full recrystallization. The same profile appearance is found in [13].

In order to compare the microhardness with TIG process, an average value has been calculated for each zone of the two processes which are illustrated in Fig. 5.

It is noted that in TIG weld, average microhardness decreases in both the HAZ (124 Hv) and the NZ (119 Hv) than BM due to fusion state reached in the material and gathering of precipitates. So, the microhardness in TIG process is higher than FSW joint. This result justifies the lowest mechanical properties obtained previously in this TIG process.
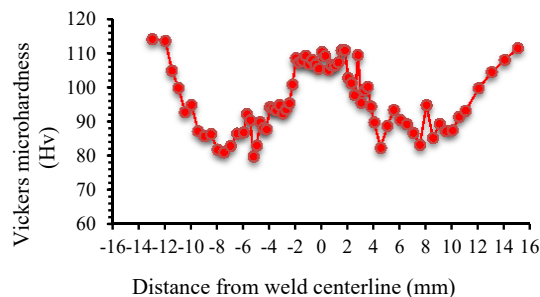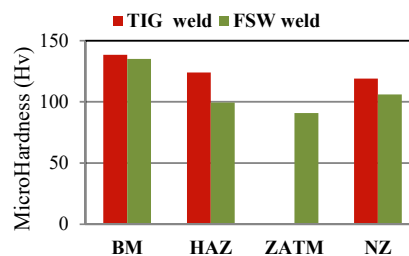
Fig. 4 FSW microhardness profile

Fig. 5 Microhardness comparison between TIG and FSW welds

Figs. 6 (a)-(c) shows the fractographs of tensile tested specimens observed in BM, FSW and TIG joints respectively. All the ruptures are produced in the HAZ for the two processes, as we have already seen. We remark the presence of round deeper dimples with different sizes and shapes. Fine dimples are characteristic feature of ductile fracture [14] and hence both FSW and TIG ruptures have shown their ductility.

From Fig. 7, the different zones of both FSW and TIG joints are displayed. We remark absence of voids, grooves and porosity, indicating the good joints quality.

As seen in Figs. 7 (a), (d)-(f), FSW exhibits four distinct zones, namely BM, HAZ, TMAZ and the NZ.
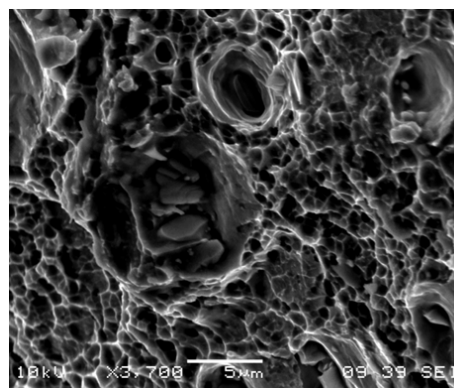

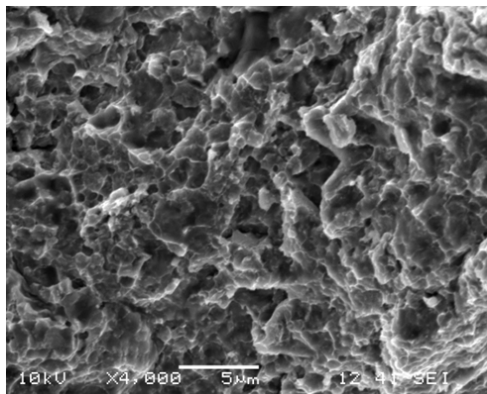Fig. 6 (a) Fracture surface in BM tensile tested specimen

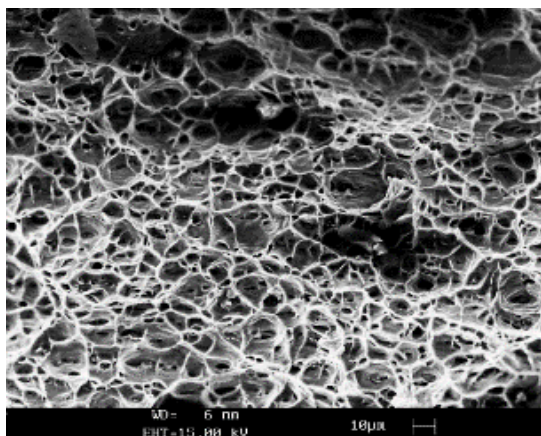Fig. 6 (b) Fracture surface in FSW tensile tested specimen

Fig. 6 (c) Fracture surface in TIG tensile tested specimen

successively fusion and solidification phases by high thermal effect.
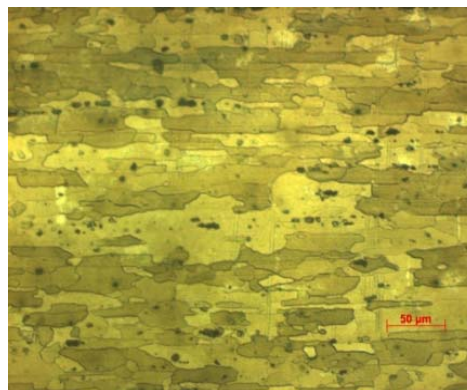

Fig. 7 (a) Microstructure of BM in FSW weld

Fig. 7 (b) Microstructure of the HAZ zone in FSW weld

Fig. 7 (c) Microstructure of the THAZ zone in FSW weld

The microstructure in the HAZ (Fig. 7 (d)), which is affected thermally but not mechanically by the tool movement, has the same appearance as that of the BM (Fig. 7 (a)) with a slightly growth in grains size. However, in the TMAZ (Fig. 7 (e)) the rotation of the tool produces material flux around the FSW tool. The grains are deformed and change direction according to deformation planes and undergo a partial recrystallization [15].

The grains within the NZ are severely deformed, equiaxed and very refined compared to grains magnitude in the BM, explaining the superior mechanical properties in this process (Fig. 7 (f)). These microstructure changes are due to the thermo-mechanical stir and full dynamic recrystallization effects. The mean grain size at the TMAZ is considerably larger than in the NZ; it measures almost double than that at the NZ.

Concerning TIG welding, the microstructures reveal three zones (BM, HAZ and NZ) (Figs. 7 (a)-(c)). Globally, the grains size is smaller in FSW than TIG. In the HAZ (Fig. 7 (b)), the grains size is also extended than BM, and it is more important compared to FSW process. This zone width is wider than FSW HAZ because of major thermal flow generated in this fusion technique. Nevertheless, the NZ (Fig. 7 (c)) is characterized by a dendritic structure and nonhomogeneous grains distribution, such as the material undergoes
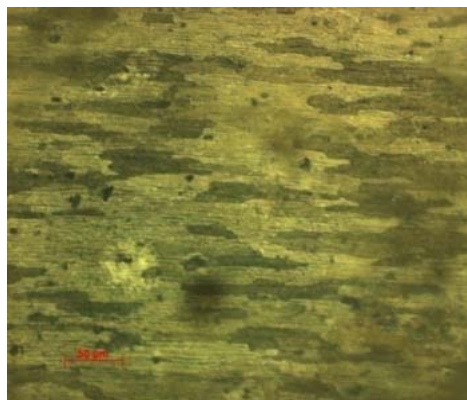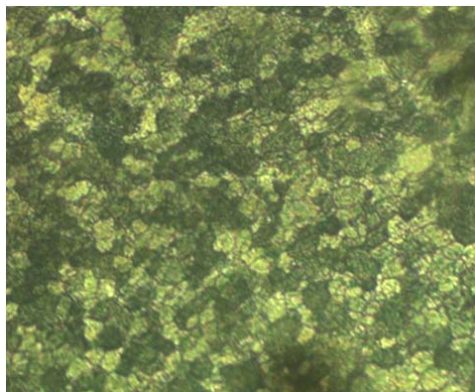
Fig. 7 (d) Microstructure of the NZ in FSW weld

Fig. 7 (e) Microstructure of the HAZ zone in TIG weld
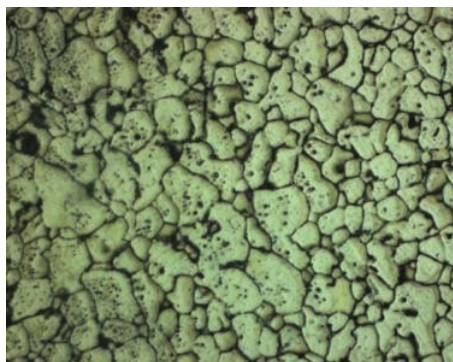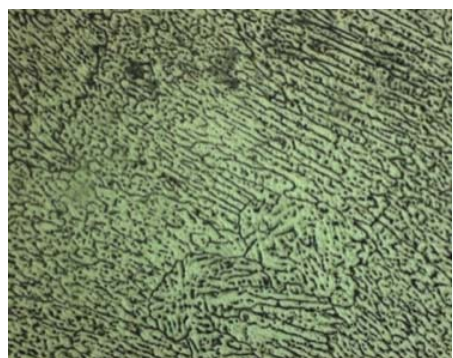

Fig. 7 (f) Microstructure of the NZ in TIG weld

IV. CONCLUSION

In the present work, two different welding techniques, FSW and TIG have been successfully applied and characterized for the welding of heat-treatable aluminium Alloy 2024-T3. The following conclusions have been drawn:

✓ The heat input and temperature picks in the case of FSW are less important than those of TIG welding process.
✓ The microhardeness decreases across the FSW weld to reach a minimal value in the TMAZ and increases in the NZ; however, in TIG process, the lowest values are localized on the NZ.
✓ A refined microstructure is obtained in FSW on the stirred zone inducing to a better tensile strength.

REFERENCES

[1] Tang, W., Guo, X., McClure, J. C., et al. 1998. "Heat input and temperature distribution in friction stir welding." J Mater Process Manuf Sci 7: pp. 163-172.
[2] Colegrove, P., Painter, M., Graham D, et al. 2000. "3 Dimensional Flow and Thermal Modeling of the Friction Stir Welding Process." In Proceedings of the 2nd International Symposium on Friction Stir Welding, Sweden.
[3] Bussu G., and Irving, P. E. 2003. "The role of residual stress and heat affected zone properties on fatigue crack propagation in friction stir welded 2024-T351 aluminium joints." Int J Fatigue 25: pp. 77-88.
[4] Thamizhmanii, S., Sukor, Sulaiman, M. A. 2013. "Solid State Friction Stir Welding (FSW) on Similar and Dissimilar Metals." In Proceedings of the World Congress on Engineering London, U.K, Vol III.
[5] Chi-Hui Chien., Wei-Bang Lin., and Thaiping Chen. 2011. "Joined and moved along the line of joining." J Chinese Inst Eng 34(1): pp. 99-105.
[6] Aissani, M., Gachi, S., and Bekache, I. 2007. "Friction Stir Welding tool (FSW)." Algerian National Institute of the patent rights 070759.
[7] Aissani, M., Gachi, S., Boubenider, F., et al. 2010. "Design and optimization of Friction Stir Welding Tool". Mater Manufact Process 25 (11): pp. 1199-1205.
[8] Buffa, G., Hua, J., Shivpuri, R., et al. 2006. "Design of the friction stir welding tool using the continuum based FEM model."Mater Sci Eng A 419(15): pp. 381-388.
[9] Mishra, RS., Ma, ZY. 2005. "Friction stir welding and processing". Mater Sci Eng R 50: pp. 1-78.
[10] Singh, H., Arora, HS. "Friction stir welding-Technology and future potential." In Proceeding of National conference on advancements and futuristic trends in mechanical and materials engineering, 2010.
[11] Hugh, R., Shercliff, a., Michae, J., et al. 2005. "Microstructural modelling in friction stir welding of 2000 series aluminium alloys." Mecanique & Industries 6: pp. 25-35.
[12] Yuh, J., Chao, X., Tang, Qi.W. 2003. "Heat Transfer in Friction Stir Welding-Experimental and Numerical Studies". Transactions of the ASME 125: pp 138.
[13] Squillace, A., Fenzo, Ade., Giorleo, G., et al. 2004. "A comparison between FSW and TIG welding techniques:modifications of microstructure and pitting corrosion resistance in AA 2024-T3 butt joints." J Mater Process Technol 152: pp. 97-105.
[14] Xu, W., Liu, J., Luan, G., et al. 2009. " Temperature evolution, microstructure and mechanical properties of friction stir welded thick 2219-O aluminum alloy joints." Mater Des 30: pp. 1886-1893.
[15] Xu, W., Liu, J., Luan, G., et al. 2009. "Microstructure and mechanical properties of friction stir welded joints in 2219-T6 aluminium alloy." Mater Des 30: pp. 3460-3467.